Research Article | Vol. 26, No. 10 | 14 May 2018 | OPTICS EXPRESS 12939

Optics EXPRESS

Strain, temperature, moisture, and transverse force sensing using fused polymer optical fibers

Arnaldo Leal-Junior,[1,*] Anselmo Frizera,[1] Heeyoung Lee,[2] Yosuke Mizuno,[2] Kentaro Nakamura,[2] Tiago Paixão,[3] Cátia Leitão,[3,4] M. Fátima Domingues,[4] Nélia Alberto,[4] Paulo Antunes,[3,4] Paulo André,[5] Carlos Marques,[4] and Maria José Pontes[1]

[1]*Telecommunications Laboratory (LABTEL), Graduate Program of Electrical Engineering of Federal University of Espírito Santo, Brazil*
[2]*Institute of Innovative Research, Tokyo Institute of Technology, Japan*
[3]*Physics Department & I3N, University of Aveiro, Portugal*
[4]*Instituto de Telecomunicações, Campus Universitário de Santiago, 3810-193 Aveiro, Portugal*
[5]*Instituto de Telecomunicações and Department of Electrical and Computer Engineering, Instituto Superior Técnico, University of Lisbon, Portugal*
[*]*arnaldo.leal@aluno.ufes.br*

Abstract: This paper presents the characterization of polymer optical fibers (POFs) submitted to the catastrophic fuse effect towards intensity-variation-based sensing of strain, transverse force, temperature, and moisture. In the experiments, POFs with and without the fuse effect are tested and the results are compared with respect to the sensitivity, linearity, and root mean squared error (RMSE). The fused POFs have higher linearity and lower RMSE than non-fused POFs in strain and transverse force sensing. Also, the sensitivity of the fused POFs is higher in transverse force and temperature sensing, which can be related to the higher sensitivity to the curvature that the transverse force creates on the POF and to the more significant variations of the refractive index with temperature increase. Additionally, the fused POFs present lower moisture absorption than the non-fused POFs. The presented results indicate a great potential of the fused POFs intensity-variation-based sensing applications of various physical parameters.

OCIS codes: (160.5470) Polymers; (130.5460) Polymer waveguides; (280.4788) Optical sensing and sensors; (060.2370) Fiber optics sensors.

References and links

1. R. Kashyap, "The fiber fuse--from a curious effect to a critical issue: A 25^th year retrospective," Opt. Express **21**(5), 6422–6441 (2013).
2. S. Todoroki, *Fiber Fuse: Light-Induced Continuous Breakdown of Silica Glass Optical Fiber* (Springer, 2014).
3. E. M. Dianov, I. A. Bufetov, A. A. Frolov, Y. K. Chamorovsky, G. A. Ivanov, and I. L. Vorobjev, "Fiber Fuse Effect in Microstructured Fibers," IEEE Photonics Technol. Lett. **16**(1), 180–181 (2004).
4. F. Domingues, A. R. Frias, P. Antunes, A. O. P. Sousa, R. A. S. Ferreira, and P. S. André, "Observation of fuse effect discharge zone nonlinear velocity regime in erbium-doped fibres," Electron. Lett. **48**(20), 1295 (2012).
5. E. M. Dianov, I. A. Bufetov, A. A. Frolov, V. M. Mashinsky, V. G. Plotnichenko, M. F. Churbanov, and G. E. Snopatin, "Catastrophic destruction of fluoride and chalcogenide optical fibres," Electron. Lett. **38**(15), 783 (2002).
6. N. Hanzawa, K. Kurokawa, K. Tsujikawa, T. Matsui, K. Nakajima, S. Tomita, and M. Tsubokawa, "Suppression of fiber fuse propagation in hole assisted fiber and photonic crystal fiber," J. Lightwave Technol. **28**(15), 2115–2120 (2010).
7. Y. Mizuno, N. Hayashi, H. Tanaka, K. Nakamura, and S. I. Todoroki, "Observation of polymer optical fiber fuse," Appl. Phys. Lett. **104**(4), 043302 (2014).
8. Y. Mizuno, N. Hayashi, H. Tanaka, K. Nakamura, and S. Todoroki, "Propagation mechanism of polymer optical fiber fuse," Sci. Rep. **4**(1), 4800 (2015).
9. Y. Mizuno, N. Hayashi, H. Tanaka, and K. Nakamura, "Spiral Propagation of Polymer Optical Fiber Fuse Accompanied by Spontaneous Burst and Its Real-Time Monitoring Using Brillouin Scattering," IEEE Photon. J. **6**, (2014).

#326203 https://doi.org/10.1364/OE.26.012939
Journal © 2018 Received 15 Mar 2018; revised 20 Apr 2018; accepted 25 Apr 2018; published 4 May 2018

Optics EXPRESS

10. P. F. C. Antunes, M. F. F. Domingues, N. J. Alberto, and P. S. André, "Optical fiber microcavity strain sensors produced by the catastrophic fuse effect," IEEE Photonics Technol. Lett. **26**(1), 78–81 (2014).
11. M. De Fátima, F. Domingues, T. De Brito Paixão, E. F. T. Mesquita, N. Alberto, A. R. Frias, R. A. S. Ferreira, H. Varum, P. F. Da Costa Antunes, and P. S. De Brito André, "Liquid hydrostatic pressure optical sensor based on micro-cavity produced by the catastrophic fuse effect," IEEE Sens. J. **15**, 5654–5658 (2015).
12. N. Alberto, C. Tavares, M. F. Domingues, S. F. H. Correia, C. Marques, P. Antunes, J. L. Pinto, R. A. S. Ferreira, and P. S. André, "Relative humidity sensing using micro-cavities produced by the catastrophic fuse effect," Opt. Quantum Electron. **48**(3), 1–8 (2016).
13. M. F. Domingues, P. Antunes, N. Alberto, R. Frias, R. A. S. Ferreira, and P. André, "Cost effective refractive index sensor based on optical fiber micro cavities produced by the catastrophic fuse effect," Meas. J. Int. Meas. Confed. **77**, 265–268 (2016).
14. M. F. Domingues, P. Antunes, N. Alberto, A. R. Frias, A. R. Bastos, R. A. S. Ferreira, and P. S. André, "Enhanced sensitivity high temperature optical fiber FPI sensor created with the catastrophic fuse effect," Microw. Opt. Technol. Lett. **57**(4), 972–974 (2015).
15. C. A. R. Díaz, C. Leitão, C. A. Marques, M. F. Domingues, N. Alberto, M. J. Pontes, A. Frizera, M. R. N. Ribeiro, P. S. B. André, and P. F. C. Antunes, "Low-Cost Interrogation Technique for Dynamic Measurements with FBG-Based Devices," Sensors (Basel) **17**(10), 2414 (2017).
16. C. A. F. Marques, D. J. Webb, and P. Andre, "Polymer optical fiber sensors in human life safety," Opt. Fiber Technol. **36**, 144–154 (2017).
17. A. R. Prado, A. G. Leal-Junior, C. Marques, S. Leite, G. L. de Sena, L. C. Machado, A. Frizera, M. R. N. Ribeiro, and M. J. Pontes, "Polymethyl methacrylate (PMMA) recycling for the production of optical fiber sensor systems," Opt. Express **25**(24), 30051–30060 (2017).
18. P. F. C. Antunes, H. Varum, and P. S. Andre, "Intensity-encoded polymer optical fiber accelerometer," IEEE Sens. J. **13**(5), 1716–1720 (2013).
19. A. G. Leal-Junior, A. Frizera, and M. J. Pontes, "Dynamic Compensation Technique for POF Curvature Sensors," J. Lightwave Technol. **36**(4), 1112–1117 (2018).
20. A. Leal-Junior, A. Frizera-Neto, C. Marques, and M. J. Pontes, "A Polymer Optical Fiber Temperature Sensor Based on Material Features," Sensors (Basel) **18**(2), 301 (2018).
21. A. G. Leal-Junior, A. Frizera, C. Marques, M. R. A. Sanchez, W. M. dos Santos, A. A. G. Siqueira, M. V. Segatto, and M. J. Pontes, "Polymer Optical Fiber for Angle and Torque Measurements of a Series Elastic Actuator's Spring," J. Lightwave Technol. **36**(9), 1698–1705 (2018).
22. D. Z. Stupar, J. S. Bajić, B. M. Dakić, M. P. Slankamenac, and M. B. Živanov, "The possibility of using a plastic optical fibre as a sensing element in civil structural health monitoring," Phys. Scr. **T157**, 014031 (2013).
23. L. Bilro, N. Alberto, J. L. Pinto, and R. Nogueira, "Optical sensors based on plastic fibers," Sensors (Basel) **12**(9), 12184–12207 (2012).
24. A. Leal-Junior, A. Frizera, M. J. Pontes, P. Antunes, N. Alberto, M. F. Domingues, H. Lee, R. Ishikawa, Y. Mizuno, K. Nakamura, P. André, and C. Marques, "Dynamic mechanical analysis on fused polymer optical fibers: towards sensor applications," Opt. Lett. **43**(8), 1754–1757 (2018).
25. A. Pospori, C. A. F. Marques, D. Sáez-Rodríguez, K. Nielsen, O. Bang, and D. J. Webb, "Thermal and chemical treatment of polymer optical fiber Bragg grating sensors for enhanced mechanical sensitivity," Opt. Fiber Technol. **36**, 68–74 (2017).
26. W. Yuan, A. Stefani, M. Bache, T. Jacobsen, B. Rose, N. Herholdt-Rasmussen, F. K. Nielsen, S. Andresen, O. B. Sørensen, K. S. Hansen, and O. Bang, "Improved thermal and strain performance of annealed polymer optical fiber Bragg gratings," Opt. Commun. **284**(1), 176–182 (2011).
27. P. Stajanca, O. Cetinkaya, M. Schukar, P. Mergo, D. J. Webb, and K. Krebber, "Molecular alignment relaxation in polymer optical fibers for sensing applications," Opt. Fiber Technol. **28**, 11–17 (2016).
28. A. G. L. Junior, A. Frizera, and M. J. Pontes, "Analytical model for a polymer optical fiber under dynamic bending," Opt. Laser Technol. **93**, 92–98 (2017).
29. N. Zhong, M. Zhao, Q. Liao, X. Zhu, Y. Li, and Z. Xiong, "Effect of heat treatments on the performance of polymer optical fiber sensor," Opt. Express **24**(12), 13394–13409 (2016).
30. N. Zhong, Q. Liao, X. Zhu, M. Zhao, Y. Huang, and R. Chen, "Temperature-independent polymer optical fiber evanescent wave sensor," Sci. Rep. **5**(1), 11508 (2015).

1. Introduction

The catastrophic fuse effect is a self-destruction process of an optical fiber, triggered when extremely high-power optical signals are injected into a fiber submitted to non-ideal conditions, such as tight bendings, and damaged connectors [1,2]. Once an optical discharge is initiated, it is trapped in the fiber core and travels back toward the light source, consuming the light energy and permanently damaging the fiber. This effect was first observed in silica single-mode fibers (SMFs) in 1987 [1]. Thereafter, the fuse effect has been continuously studied in different glass fibers, including micro structured [3], erbium-doped [4], fluoride [5], chalcogenide [5], and photonic crystal [6]. Recently, the fuse effect has been observed

Optics EXPRESS

and characterized in polymer optical fibers (POFs) [7–9]. At 1550 nm, the propagation velocity of the POF fuse was estimated to be approximately 20 mm/s (one to two orders slower when compared with silica fiber fuse), and the threshold power density was 6.6 kW/cm^2 (>150 times lower than that of the silica fiber fuse) [7]. The temperature of the optical discharge was estimated to be ~3600 K, which was much lower than for the silica fiber fuse [8]. Thus, the physical properties of the POF fuse are unique.

The fuse effect in silica SMFs produces voids along the fibers, which can be used as a cost-effective alternative for Fabry-Perot interferometry (FPI) [10]. For this reason, fused silica SMFs have been employed in sensing applications of strain [10], liquid level [11], relative humidity [12], refractive index [13], and temperature [14]. Another application of the fused silica SMFs is as an edge filter for low-cost interrogation of fiber Bragg gratings [15].

Although the referred voids are also observed in fused POFs, they formation are not stable [8], which may inhibit their applications as FPI micro-cavities. However, the POFs in which the fuse effect occurred (fused POFs) have a unique advantage, since the optical propagation loss is lower than the values for the fused silica SMFs. This optical propagation loss value for the fused POFs is approximately 1.4 dB/cm, which is adequate to enable the signal propagation for a few centimeters [7,8]. In addition, POFs present advantages over silica SMFs regarding their material features, such as higher strain limit, fracture toughness, and resistance to impact loads [16]. Therefore, fused POFs could be applicable to physical sensing with new approaches, different from the ones used with the fused silica SMFs.

One possible interrogation technique for fused-POF-based sensors is to exploit the light intensity variations with respect to physical parameters, such as refractive index [17], acceleration [18], angle [19], temperature [20], torque [21], and strain [22]. Intensity-variation-based fiber-optic sensors generally present the advantages of cost efficiency and simplicity of signal processing [23]. Recently, a dynamic mechanical analysis on the fused and non-fused POFs has been performed [24], and the fused POFs have been shown to be potentially higher in performance for strain sensing applications.

Considering this background, here we characterize the fused POFs for strain and transverse force sensing. The response of the fused POFs to these parameters are compared with those of the same POFs without the fuse effect. Subsequently, both fused and non-fused POFs are also characterized with respect to temperature and moisture absorption, in order to evaluate the cross-sensitivity of the strain and transverse force sensors to these environmental parameters.

2. Experimental setup

The POF employed in the experiment had a perfluorinated graded-index core with 50 μm diameter made of doped polyperfluorobutenylvinyl ether, a cladding of the same material without doping with 25 μm thickness, and an overcladding (composed of polycarbonate) that resulted in an outer diameter of 750 μm. The fuse was initiated using the experimental setup and methods described by Y. Mizuno *et al* [7], where there is an amplified optical power of 200 mW injected into the POF that presents one end connected to a silica single mode fiber using an FC/SC adaptor and the other end polished with a 0.5 μm alumina powder for the fuse effect ignition. Since fused POFs have much higher optical propagation loss than non-fused POFs (0.25 dB/m at 1550 nm for fused POFs, where the one for non-fused POF is about 250 dB/km), the length of the fused and non-fused POF samples was set to 3.4 cm, for a reliable performance comparison.

In order to reduce the internal stress generated during the fiber drawing process and to enhance its mechanical sensitivity [25], the annealing was performed to both the fused and non-fused POF samples. Using a thermostatic chamber (1/400 ND, Ethik Technology), the temperature around the samples were maintained at 95°C (close to their glass transition temperatures) for 48 hours [26], where the annealing time chosen is large enough to guarantee the molecular alignment relaxation required for the Young's modulus reduction [27]. After

Optics EXPRESS

preparation of the samples, they were installed in the setup presented in Fig. 1(a) for strain tests. One end of the POF was fixed, with acrylate glue, on a fixed stage and the other on a translation stage with controllable displacements. The applied displacements resulted in a strain ranging from 0.5 to 1.5%. For transverse force tests, another setup depicted in Fig. 1(b) was used. Calibrated weights corresponding to transverse forces of 5, 10, 15, and 20 N were applied to each POF sample installed in the setup. It is worth to mention that higher forces can be applied in the fiber, if its strain limit (~8%) is not surpassed. However, these forces were not applied due to experimental limitations of the employed setup.

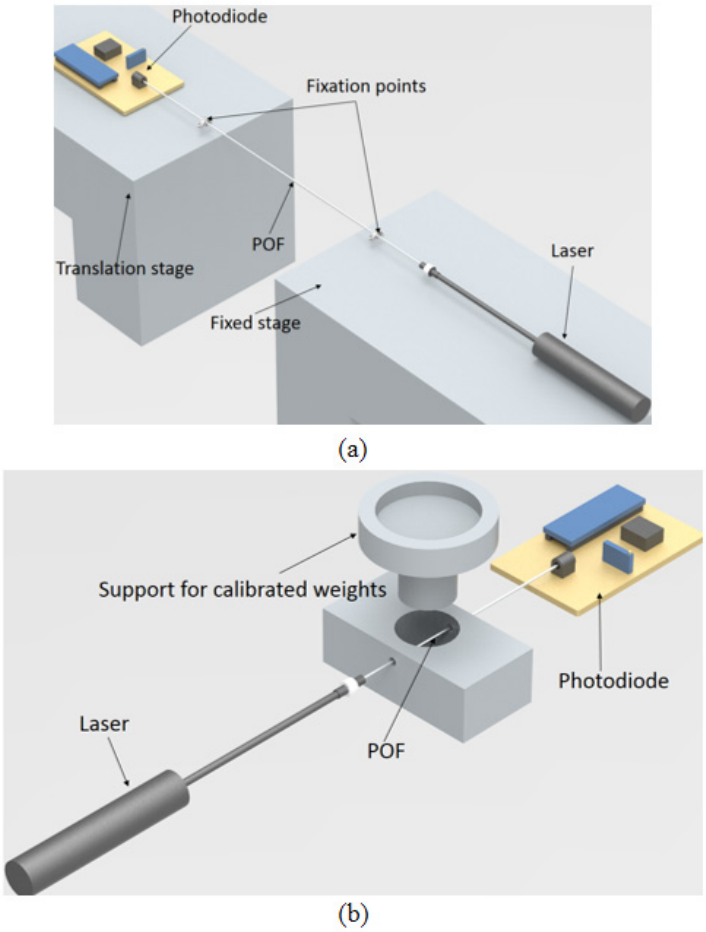

Fig. 1. Schematics of the experimental setups for (a) strain and (b) transverse force characterizations of fused and non-fused POFs.

The optical signal source was a low-cost laser peaking at 650 nm with an optical power of 5 mW. The signal acquisition was performed with a photodetector (IF-D91, Industrial Fiber Optics) with a trans-impedance amplifier, which was connected to an acquisition board (USB-6008, National Instruments) for signal acquisition at 200 Hz. Regarding the temperature characterization, the POF samples were placed over a thermoelectric Peltier plate (TEC1-12706, Hebei IT) with a temperature controller (TED 200 C, Thorlabs). Using a similar setup as depicted in Fig. 1, the optical power transmitted through the POF was measured continually, at 25, 30, 40, and 50°C, for a period of 3 hours. The temperature upper limit (50°C) is the highest temperature of the Peltier plate employed. Nevertheless, the sensor is able to operate in higher temperatures, where the temperature limitation is the fiber glass

Optics EXPRESS

transition temperature. The moisture absorption was also evaluated by immersing each POF sample inside a container filled with distilled water. Both samples were straightly placed to avoid the optical loss caused by bending.

3. Results and discussion

The strain characterization results are shown in Fig. 2. The transmitted optical power, through the fused and non-fused POF samples, were plotted as function of the applied strain. The transmitted optical power (in mW) was normalized using its zero-strain value as a reference. The error bars were defined as the standard deviations of the three measurements under the same condition. With increasing strain, both samples exhibited almost linear negative dependencies, with correlation factor closers to the unit. The strain sensitivity of the non-fused POF was approximately 1.4 times higher than that of the fused POF, while the fused POF had higher linearity. The root mean squared errors (RMSEs) between the reference strain applied and the one measured by the POF sensors for the fused and non-fused POFs with respect to the strain were 0.002% and 0.111%, respectively. In this case, the reference strain is the translation stage axial movement divided by the initial fiber length.

One possible reason for the high linearity of the fused POF is the linear relation between stress and strain in this strain range. When the POF is under strain, it is induced stress, leading to the variations of its refractive index due to the stress-optic effect, which generally induces changes on the transmitted power due to the variation of the critical angle and number of modes [28]. Thus, the linear deviations on the fiber stress may lead to linear variations of the POF power, which can also explain the lower errors of the fused POF. In contrast, the lower sensitivity of the fused POF can be explained assuming that both POFs are in the elastic regions, by the Hooke's law presented in Eq. (1).

$$\sigma = \mathrm{E}\,\varepsilon, \tag{1}$$

where σ is the stress, E is the Young's modulus, and ε is the strain. This equation indicates that, if submitted to the same strain, the material with a lower Young's modulus has lower stress than that with a higher Young's modulus. As it has been reported in [24], the fused POF has a smaller value of Young's modulus, therefore the stress on the POF becomes lower, leading to lower power attenuation than the non-fused POF. For this reason, the fused POF presented a lower sensitivity ($0.0042\%^{-1}$) than the one of non-fused POFs ($0.0060\%^{-1}$), but with higher linearity (0.999 for the fused POF and 0.985 for the non-fused ones) and, consequently, lower errors.

Optics EXPRESS

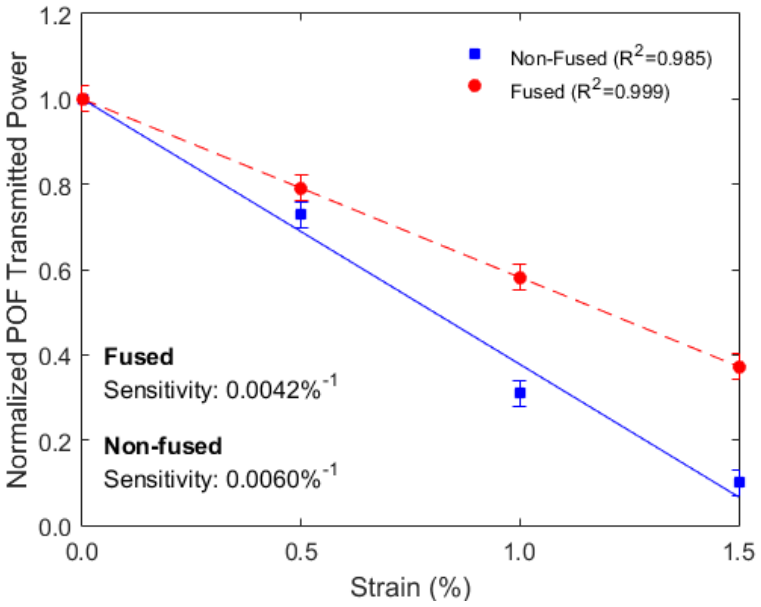

Fig. 2. Normalized transmitted optical power plotted as function of strain applied to fused (red) and non-fused (blue) POFs. The points are experimental data, and the lines are linear regressions.

Subsequently, the transmitted power dependence on the transverse force is shown in Fig. 3. The transmitted optical power was normalized using as a reference the situation without loading. The force sensitivity of the fused POF was approximately 1.3 times higher than that of the non-fused POF. The sensitivity of fused POFs is 0.024 N^{-1}, whereas the non-fused POFs presented a sensitivity of about 0.019 N^{-1}. The force sensitivity is related to the curvature that the POFs are subjected when the force is applied, and the higher force sensitivity of the fused POF is probably originated from its higher sensitivity to curvature. Additionally, the fused POF also presented higher linearity than that of the non-fused POF, which seems to be related to the linear stress-strain relation of the fused POF. The RMSE for the non-fused POFs with respect to the transverse force was 0.64 N, while that for the fused fibers was 0.27 N. Therefore, the fused POF has been shown to have many advantages over the non-fused POF for transverse force sensing applications, including higher sensitivity, higher linearity, and lower measurement error. Furthermore, the non-fused POF presented a nonlinear behavior under transverse force with a linearity of 0.923. This low linearity also leads to a normalized transmitted power higher than 1 in the linear regression curve when the force is zero. Thus, it is only related to the sensor nonlinearity, since the measured value at zero force is 1 for both sensors.

Optics EXPRESS

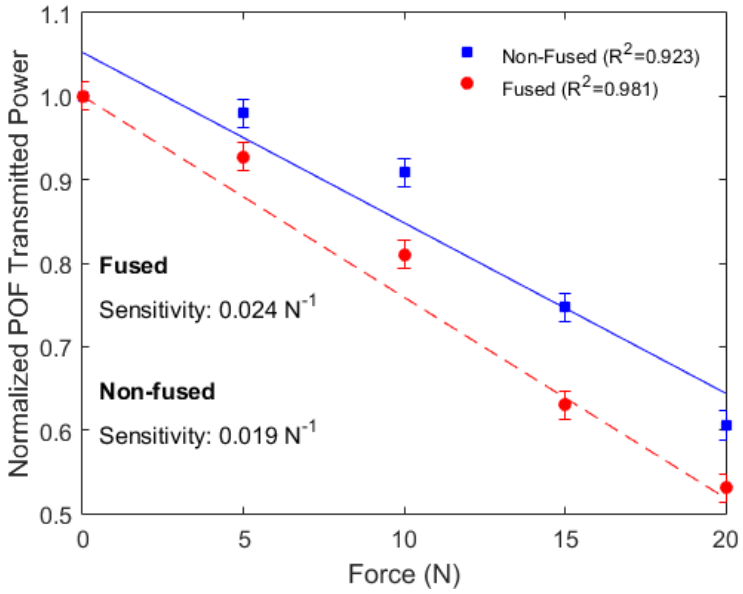

Fig. 3. Normalized transmitted optical power plotted as a function of transverse force applied to fused (red) and non-fused (blue) POFs. The points are experimental data, and the lines are linear regressions.

The transmitted optical power with respect to temperature was also measured as is shown in Fig. 4. The transmitted optical power was normalized using as a reference its value at 25°C. With increasing temperature, the POF optical propagation loss increases, irrespective of the samples, but the temperature sensitivity of the fused POF was >20 times higher than the non-fused POF. The intensity variation obtained with the temperature increase is related to the thermo-optic effect, which is the POF refractive index variation with respect to the temperature, as characterized in [29]. Although the fused POFs did not exhibit a sharp decrease in the Young's modulus at temperature close to the glass-transition temperature, they showed larger variations of the Young's modulus at temperature of <60°C than those of the non-fused POFs [24]. Therefore, there might be larger power variations in the fused POFs due to thermally induced strain. In addition, the temperature increase generally causes variations of the refractive index, resulting in deviations of the transmitted power [30]; such variations may be larger in the fused POFs. Thus, the fused POFs presented a sensitivity more than 10 times higher when compared with the non-fused POFs, where the sensitivities are 0.016 $°C^{-1}$ and 0.0014 $°C^{-1}$ for the fused and non-fused POFs, respectively. The lower linearity of the fused POF (0.976 for the fused and 0.985 for non-fused ones) may be attributed to the nonlinearity of the refractive index variations with temperature, which also leads to larger measurement errors [30].

Optics EXPRESS

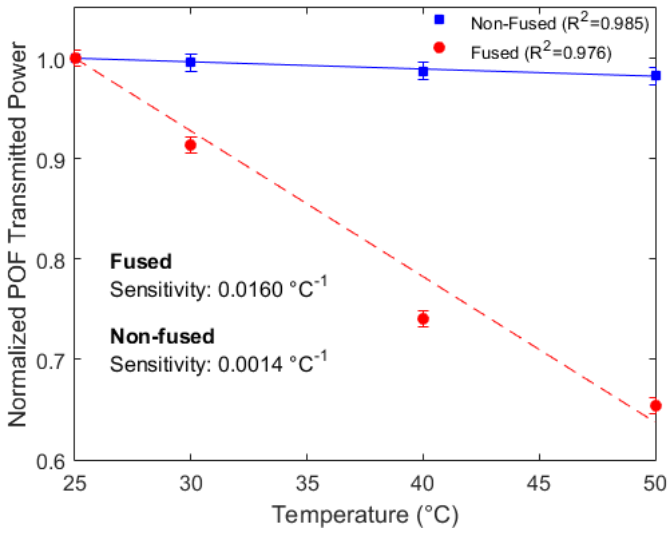

Fig. 4. Fused (red) and non-fused (blue) POF response to temperature (points are experimental data, and the lines are linear regressions).

Finally, the moisture absorption of the POF samples was evaluated. Figure 5 shows the normalized transmitted power of the fused and non-fused POFs plotted as functions of time. Both POF samples showed significant power reduction within 20 minutes subsequently to their immersion in distilled water at 25°C. After that period, the transmitted power became relatively stable. Regardless of time, the variations of the normalized transmitted power of the non-fused POF (maximum: 10.8%) were larger than those of the fused POF (maximum: 7.8%), which indicates that fused POF absorbs less water. Such lower variations can be ascribed to the lower sensitivity to humidity [24]. Additionally, the fused POFs presented a higher stability than the non-fused ones after 30 minutes, where the standard deviation in the interval from 30 minutes to 180 minutes is 2.03% for the non-fused and 0.12% for the non-fused POFs.

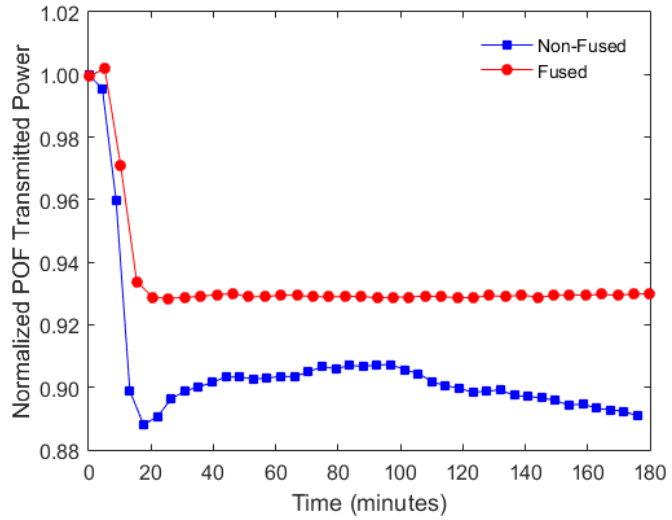

Fig. 5. Fused (red) and non-fused (blue) POF response to time after the POFs were immersed into distilled water.

Optics EXPRESS

4. Conclusions

We characterized the fused POF as a candidate of an intensity-variation-based sensing element for strain and transverse force, as well as temperature and moisture absorption. The fused POF showed 1.4 times smaller dependence on strain than that of the non-fused POF, but their sensitivities to transverse force and temperature were 1.3 times and >20 times higher than those of non-fused POFs, respectively. The linearity and measurement error were also evaluated. In addition, the moisture absorption of the fused POF was lower than that of the non-fused POF. These results prove the advantages of the fused POF as an element of intensity-variation-based sensors, especially for highly sensitive transverse force and temperature sensing. We foresee the use of these properties on the development of interferometry-based sensors and the use of the electric conductivity of the fused POF [8] may lead to the development of novel sensing systems. In addition, future works also include the inscription of short or long period gratings in the fused POF, where the core carbonization due to the fuse can be a kind of hollow core fiber.

Funding

Coordenação de Aperfeiçoamento de Pessoal de Nível Superior (CAPES) (88887.095626/2015-01); Fundação Estadual de Amparo à Pesquisa do Estado do Espírito Santo (FAPES) (72982608); Conselho Nacional de Desenvolvimento Científico e Tecnológico (CNPq) (304192/2016-3 and 310310/2015-6); Fundação para a Ciência e a Tecnologia (FCT) (PD/BD/128265/2016 (DAEPHYS), SFRH/BPD/101372/2014, and SFRH/BPD/109458/2015); Fundação para Ciência e a Tecnologia / Ministério da Educação e Ciência (UID/EEA/50008/2013); European Regional Development Fund (PT2020 Partnership Agreement); JSPS KAKENHI (17H04930 and 17J07226); Fujikura Foundation; Japan Association for Chemical Innovation; FCT, IT-LA (PREDICT scientific action).